Bystander Effects on Carbene Rearrangements: A Computational Study

Brian T. Hill,* Zhendong Zhu, Aaron Boeder, Christopher M. Hadad,* and Matthew S. Platz*

Department of Chemistry, The Ohio State University, 100 West 18th Avenue, Columbus, Ohio 43210

Received: January 16, 2002; In Final Form: March 18, 2002

Methylcarbene, dimethylcarbene, chloromethylcarbene, and *tert*-butylmethylcarbene were studied at the HF/6-31G*, MP2/6-31G*, B3LYP/6-31G*, MP2/6-31+G(2d,p), QCISD(T)/6-31G*//MP2/6-31G*, and QCISD(T)/6-31+G(2d,p) levels. Minimum energy geometries of the singlet and triplet states of the carbenes were calculated. The barriers to 1,2-hydrogen migration for $CH_3C{-}X \rightarrow CH_2{=}CHX$ were calculated and found to increase for X = Cl > CH_3 > $C(CH_3)_3$ > H. Isodesmic calculations indicate that the effect of the bystander group is to stabilize differentially the carbene reactant, thereby increasing the barrier to rearrangement for X = Cl > CH_3 > $C(CH_3)_3$ > H.

I. Introduction

Examples of bimolecular reactions of alkyl- and dialkylcarbenes are relatively rare. Photolysis of nitrogenous precursors of alkyl- and dialkylcarbenes in the presence of carbene traps (alkenes, amines, alcohols, etc.) generally produces formal products of unimolecular carbene rearrangement.[1] As these formal rearrangement reactions are exceptionally exothermic, it is a straightforward conclusion that the absolute rate constants of rearrangement of alkyl- and dialkylcarbenes must be exceptionally large ($k_R > 10^{10-11}$ s^{-1}, $\tau < 10-100$ ps, Scheme 1),

SCHEME 1

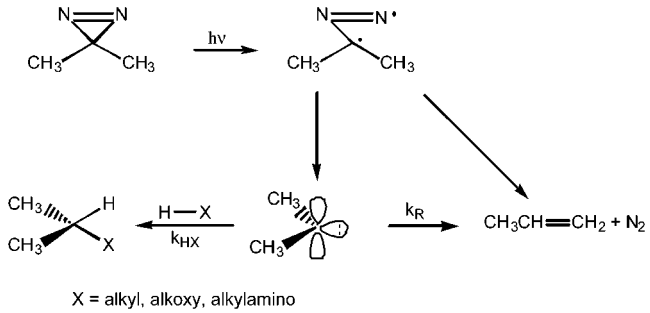

and that carbene rearrangement is much faster than bimolecular capture.

Laser flash photolysis studies indicate that dialkylcarbenes have lifetimes on the order of nanoseconds and that $k_{HX}[HX] > k_R$ (Scheme 1).[2] To reconcile the chemical and kinetic data, it has been proposed that nitrogenous precursors form carbenes inefficiently upon photochemical activation and that some, or even most, of the formal rearrangement products are produced via the electronically excited state of the precursor.[3] Calculations indicate that the rearrangements do not proceed in concert with nitrogen extrusion upon thermolysis of diazo compounds.[4,5]

Indeed, the only two ground-state singlet dialkylcarbenes yet isolated in cryogenic matrixes are adamantanylidene and dicyclopropylcarbene.[6]

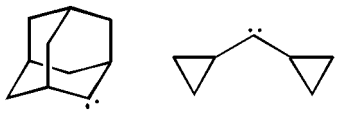

In the former species, hydrogen atoms β to the carbene center are poorly disposed toward rearrangement and the product of 1,2-hydrogen migration, adamantene, is highly strained. In the latter case, the carbene center is stabilized by overlap with the Walsh orbitals of the cyclopropane rings. Di-*tert*-butylcarbene and diadamantylcarbene[7]

have triplet ground states due to the wide bond angle at the carbene center and do not undergo 1,2-hydrogen migration. These carbenes have been detected by low-temperature EPR spectroscopy as persistent species.

Laser flash photolysis experiments have begun to reveal the influence of structure on the rate of carbene rearrangement. Bystander effects on the rate of rearrangement, first proposed by Nickon,[8] have been observed experimentally[9] and validated computationally.[5] Keating, Garcia-Garibay, and Houk[5] have demonstrated that alkylation of the carbon bearing the migrating hydrogen lowers the barrier to 1,2-hydrogen migration of alkylchlorocarbenes.

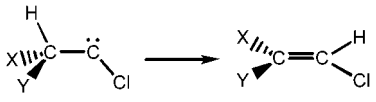

X = Y = CH_3 > X = CH_3, Y = H > X = Y = H

These results have stimulated renewed interest on the part of theory to calculate barrier heights for these rearrangements. To better appreciate the bystander effect, we have undertaken this study, which calculates prototypical alkyl-, dialkyl-, and alkylchlorocarbenes with a common set of computational methods. In this study, the bystander group X is directly bonded to the carbene center and its influence on the barrier to 1,2-hydrogen

* Corresponding authors. Email: platz.1@osu.edu; bhill@chemistry.ohio-state.edu. Phone: (614) 292-0410 (M.S.P.); (614) 292-6718 (B.T.H.). Fax (614) 292-5151.

10.1021/jp020108w CCC: $22.00
Published on Web 04/24/2002

TABLE 1: Calculated Relative Energies (kcal/mol) of Methylcarbene (MC)[a]

	HF/6-31G*	MP2/6-31G*	B3LYP/6-31G*	MP2/6-31+G(2d,p)	QCISD(T)/6-31G*//MP2/6-31G*[b]	QCISD(T)/6-311+G**//B3LYP/6-31G*[c]	QCISD(T)/6-31+G(2d,p)[d]
MC-S (C_1)	0.0	0.0	0.0	0.0	0.0	0.0	0.0
MC-T (C_s)	−25.6	−12.5	−6.6	−8.3	−8.6	−5.5	−4.4
TS1 (C_1)	12.8	1.1	2.6	−0.5	3.8	1.9	2.1
ethene (D_{2h})	−66.1	−80.4	−74.2	−78.0	−76.7	−73.0	−74.3

[a] Relative energies include scaled zero-point vibrational energy (ZPVE) corrections and are reported at 0 K. Enthalpies at 298 K relative to **MC**-S at the HF/6-31G(d), B3LYP/6-31G(d), and MP2/6-31G(d) levels are listed in the Supporting Information. See Figure 1 for structures. [b] Single-point energies include ZPVE computed at the MP2/6-31G* level. [c] Single-point energies include ZPVE computed at the B3LYP/6-31G* level. [d] The relative energies at QCISD(T)/6-31+G(2d,p) were computed using the additivity approximation: $\Delta E = \Delta E$[QCISD(T)/6-31G*//MP2/6-31G*] + ΔE[MP2/6-31+G(2d,p)] − ΔE[MP2/6-31G*] and include the scaled MP2/6-31G* ZPVE corrections.

migration within the methyl group is systematically examined. Herein, we are pleased to report our results.

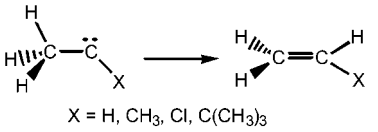

II. Computational Methods

All ab initio and density functional theory (DFT) geometry optimizations as well as analytical vibrational frequencies at the HF/6-31G*, MP2/6-31G*, and B3LYP/6-31G* levels were carried out with the GAUSSIAN94 suite of programs.[10a] Zero-point vibrational energy (ZPVE) corrections were scaled by 0.9135, 0.9670, and 0.9806 for the HF/6-31G*, MP2/6-31G*, and B3LYP/6-31G* geometries, respectively.[10b] The relative energies estimated at the QCISD(T)/6-31+G(2d,p) level were obtained using an additivity scheme that combines single-point energies computed at QCISD(T)/6-31G*, MP2/6-31+G(2d,p), and MP2/6-31G* levels using geometries optimized at the MP2/6-31G* level.[10c,d] In the cases of methylcarbene, dimethylcarbene, and chloromethylcarbene, single-point energies were also directly computed at the QCISD(T)/6-311+G** level using geometries optimized at the B3LYP/6-31G* level.

The relative energies (ΔH_0) reported in the discussion include the scaled zero-point vibrational energy (ZPVE) but do not include any thermal corrections for enthalpies at 298 K. Tables with the ΔH_{298} relative energies can be found in the Supporting Information. Singlet−triplet energy separations reported in the discussion are positive to indicate a triplet ground state according to convention. However, triplet ground states are reported with negative relative energies in the tables as the most stable singlet state is set to 0.0 kcal/mol in each case. Calculations of triplet states did not suffer from spin contamination. The expectation value of $\langle S^2 \rangle$ ranged from 2.005 to 2.021 at all levels of theory.

III. Results

III.1. Methylcarbene (MC). Methylcarbene (**MC**) has been studied extensively by computational methods and most recently by Evanseck and Houk (EH),[11] Khodabandeh and Carter (KC),[12] Gallo and Schaefer (GS),[13] and Matzinger and Fülscher (MF).[14] Single determinant methods have been shown to adequately describe alkylcarbenes and thereby justify the methods employed here.[14]

As shown in Table 1, the triplet is calculated to be the ground state by all computational methods employed in this study. The QCISD(T)/6-311+G**//B3LYP/6-31G* + ZPVE result is our most reliable estimate of the singlet−triplet (S−T) energy gap of 5.5 kcal/mol. It is comparable to the singlet−triplet separation as calculated by GS[13] (5.2 kcal/mol, CISD + DVD/TZ + 2P + f//CISD/DZP + ZPVE). However, second-order multireference

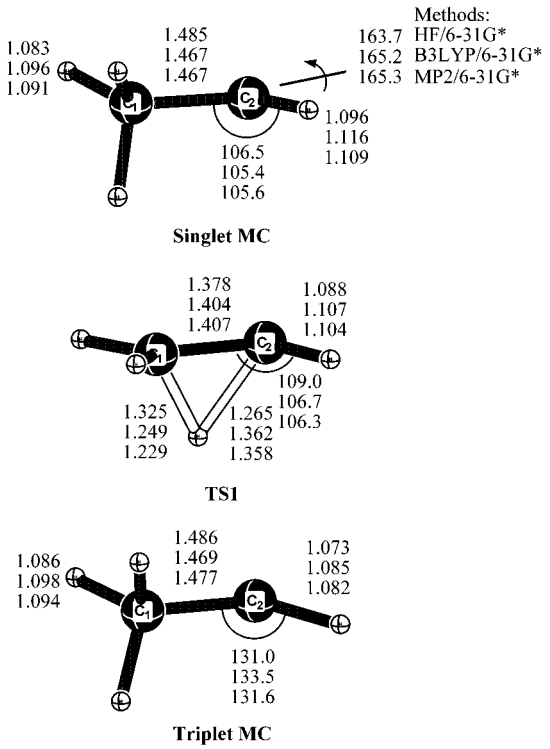

Figure 1. Optimized structures and some geometric parameters for methylcarbene (**MC**). Bond distances are in Å, and angles are in degrees.

configuration interaction calculations by MF[14] indicate a smaller singlet−triplet separation of 3.1 kcal/mol (MRCI + Q/ANO + ZPVE). Singlet **MC** was optimized in C_1 symmetry, while the triplet carbene was optimized in C_s symmetry. Optimized structures of singlet and triplet **MC** are presented in Figure 1.

The QCISD(T)/6-311+G**//B3LYP/6-31G* + ZPVE barrier for the rearrangement of singlet **MC** to ethylene is 1.9 kcal/mol. This is comparable to the barrier computed by Evanseck and Houk[11] (0.6 kcal/mol, MP4/6-311G**//MP2/6-31G* + ZPE) and by Ma and Schaefer[15] (1.2 kcal/mol, CCSD(T)/TZ2P + f). Methylcarbene has been trapped by carbon monoxide at 10 K and in solution but has never been directly observed even at cryogenic temperatures.[16] Perdeuteriomethylcarbene (CD_3CD) has been studied by the pyridine ylide method, which indicates that the apparent enthalpic barrier to its rearrangement is between 0 and 2 kcal/mol.[17] Quantum mechanical tunneling may contribute to the kinetics of rearrangement of **MC** (vide infra), as deduced for dimethylcarbene.[2]

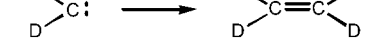

III.2. Dimethylcarbene (DMC). A single methyl group decreases the S−T gap from 9.0 kcal/mol (CH_2) to ∼3

TABLE 2: Calculated Relative Energies (kcal/mol) of Dimethylcarbene (DMC)[a]

	HF/6-31G*	MP2/6-31G*	B3LYP/6-31G*	MP2/6-31+G(2d,p)	QCISD(T)/6-31G*//MP2/6-31G*[b]	QCISD(T)/6-311+G**//B3LYP/6-31G*[c]	QCISD(T)/6-31+G(2d,p)[d]
DMC-S (C_2)	0.0	0.0	0.0	0.0	0.0	0.0	0.0
DMC-T (C_{2v})	−21.0	−5.8	−1.9	−1.4	−3.0	0.04	1.4
TS2 (C_1)	18.5	6.5	8.4	5.0	9.1	7.3	7.6
propene (C_s)	−60.3	−72.9	−66.2	−70.6	−69.3	−65.8	−67.0

[a] Relative energies include scaled zero-point vibrational energy (ZPVE) corrections and are reported at 0 K. Enthalpies at 298 K relative to **DMC**-S at the HF/6-31G(d), B3LYP/6-31G(d), and MP2/6-31G(d) levels are listed in the Supporting Information. See Figure 2 for structures. [b] Single-point energies include ZPVE computed at the MP2/6-31G* level. [c] Single-point energies include ZPVE computed at the B3LYP/6-31G* level. [d] The relative energies at QCISD(T)/6-31+G(2d,p) were computed using the additivity approximation: $\Delta E = \Delta E$[QCISD(T)/6-31G*//MP2/6-31G*] + ΔE[MP2/6-31+G(2d,p)] − ΔE[MP2/6-31G*] and include the scaled MP2/6-31G* ZPVE corrections.

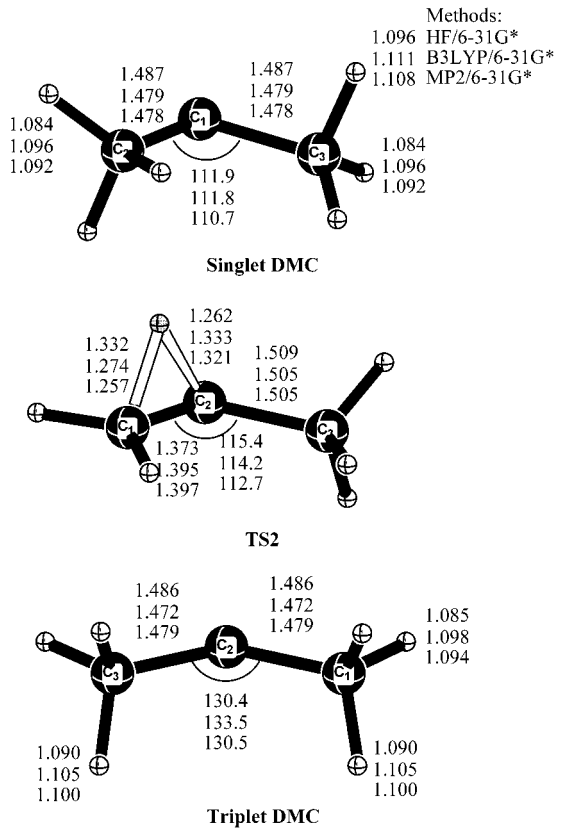

Figure 2. Optimized structures and some geometric parameters for dimethylcarbene (**DMC**). Bond distances are in Å, and angles are in degrees.

kcal/mol (CH_3-C-H); thus it is not surprising that a second methyl group reduces the S−T splitting of **DMC** even further. Singlet **DMC** was optimized in C_2 symmetry, while triplet **DMC** was optimized with C_{2v} symmetry. The optimized geometries are presented in Figure 2, and the relative energies of minima and transition states are listed in Table 2. The S−T energy separation was found to be 1.4 kcal/mol at the CCSD(T)/TZ2P + f + ZPVE level by Richards et al.[18] and 1.64 kcal/mol (MRCI + Q/ANO + ZPVE) by MF.[14] We calculate that the S−T separation becomes progressively smaller utilizing the HF/6-31G*, MP2/6-31G*, B3LYP/6-31G*, MP2/6-31+G(2d,p), and QCISD(T)/6-311+G**//B3LYP/6-31G* methods (Table 2). QCISD(T)/6-31G*//MP2/6-31G* results deviate from this trend, suggesting that the S−T separation is 3.0 kcal/mol. While the smallest S−T gap (0.04 kcal/mol) at QCISD(T)/6-311+G**//B3LYP/6-31G* indicates isoenergetic singlet and triplet states in **DMC**, the additivity approximation to QCISD(T)/6-31+G(2d,p) indicates that singlet **DMC** is the ground state by 1.4 kcal/mol.

The second methyl group is predicted to exert a substantial bystander effect on the barrier to 1,2-H migration in dimethylcarbene. Previously, the barrier to 1,2-H migration of **DMC** was calculated to be 4.7 kcal/mol by Evanseck and Houk[19] (MP2/6-31G*//RHF/6-31G* + corrections) and 7.4 kcal/mol (CCSD(T)/ANO + ZPE) by Ford et al.[2] Our "best" calculation of the barrier height for the 1,2-H migration of **DMC** is 7.3 kcal/mol at the QCISD(T)/6-311+G**//B3LYP/6-31G* level although the additivity approximation led to a similar value (7.6 kcal/mol). As shown in Figure 2, a greater structural distortion is required between singlet **DMC** and the transition state for the 1,2-H migration (**TS2**) than is the case for **MC**. This required distortion is partially responsible for the increased activation barrier for 1,2-hydrogen migration in **DMC** relative to **MC**. Differential stabilization of the singlet carbene reactant upon substitution of CH_3 for H will be shown to be the major origin of the increased barrier height. Indeed, isodesmic reactions of the form

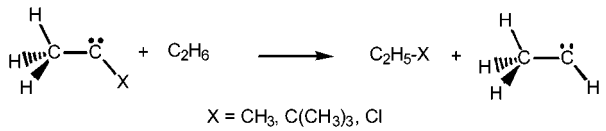

indicate that the singlet stabilization energy (SSE) of a methyl group is 9−10 kcal/mol. That is, singlet methylcarbene is stabilized by nearly 9−10 kcal/mol upon substitution of H with CH_3.

Ford et al.[2] found that the experimental barriers to 1,2-H migration of **DMC** and **DMC**-d_6 in perfluorohexane were 2.6 and 5.6 kcal/mol, respectively. It was concluded that quantum mechanical tunneling (QMT) contributes substantially to the 1,2-H migration of **DMC**, which lowers the apparent barrier to rearrangement. The barrier to rearrangement of **DMC**-d_6, where tunneling will be less important than in **DMC**, is in reasonable agreement with the theoretical calculations. The lower than expected barrier in **DMC**-d_6 suggests that there may still be a contribution of QMT to the 1,2-D migration in **DMC**-d_6.

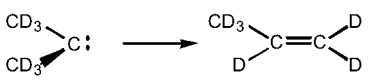

The computed barrier to the 1,2-H migration in **DMC** is 5−6 kcal/mol greater than that of **MC**, and experimentally, the barrier to rearrangement of **DMC**-d_6 is ∼4 kcal/mol larger than that of **MC**-d_4, where tunneling effects will be less important than in the parent isotopomers.

III.3. Chloromethylcarbene (CMC). Chloromethylcarbene has bountiful bimolecular chemistry. It is formed efficiently from the corresponding diazirine, and its reactions with alkenes have large absolute bimolecular rate constants. Its lifetime in alkane solvent at ambient temperature is hundreds of nanoseconds.[9] It

TABLE 3: Calculated Relative Energies (kcal/mol) of Chloromethylcarbene (CMC)[a]

	HF/6-31G*	MP2/6-31G*	B3LYP/6-31G*	MP2/6-31+G(2d,p)	QCISD(T)/6-31G*//MP2/6-31G*[b]	QCISD(T)/6-311+G**//B3LYP/6-31G*[c]	QCISD(T)/6-31+G(2d,p)[d]
CMC-S (C_1)	0.0	0.0	0.0	0.0	0.0	0.0	0.0
CMC-T (C_s)	−14.2	2.8	6.5	7.3	6.0	8.4	10.5
TS3 (C_1)	21.9	12.1	13.5	10.4	15.1	13.1	13.4
chloroethene (C_s)	−52.4	−62.6	−56.0	−59.7	−58.2	−55.2	−55.3

[a] Relative energies include scaled zero-point vibrational energy (ZPVE) corrections and are reported at 0 K. Enthalpies at 298 K relative to **CMC**-S at the HF/6-31G(d), B3LYP/6-31G(d), and MP2/6-31G(d) levels are listed in the Supporting Information. See Figure 3 for structures. [b] Single-point energies include ZPVE computed at the MP2/6-31G* level. [c] Single-point energies include ZPVE computed at the B3LYP/6-31G* level. [d] The relative energies at QCISD(T)/6-31+G(2d,p) were computed using the additivity approximation: $\Delta E = \Delta E$[QCISD(T)/6-31G*//MP2/6-31G*] + ΔE[MP2/6-31+G(2d,p)] − ΔE[MP2/6-31G*] and include the scaled MP2/6-31G* ZPVE corrections.

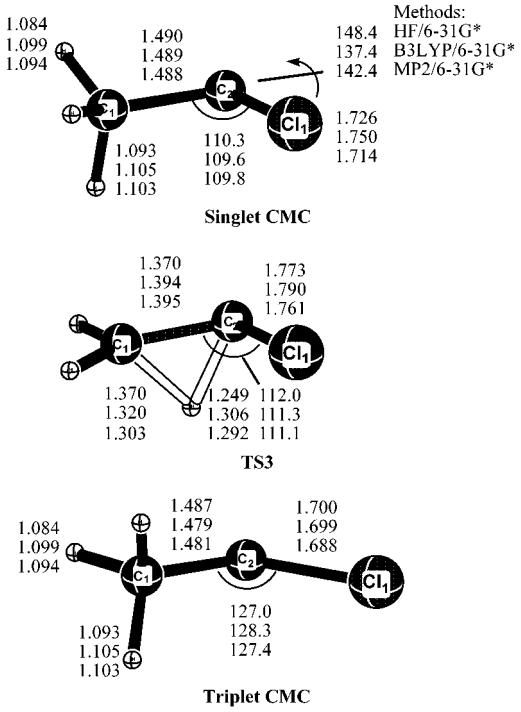

Figure 3. Optimized structures and some geometric parameters for chloromethylcarbene (**CMC**). Bond distances are in Å, and angles are in degrees.

is thought to have a singlet ground state as it reacts sluggishly with molecular oxygen. This is understood intuitively as a consequence of the donation of a pair of nonbonding electrons on chlorine into the empty p orbital of the carbene.

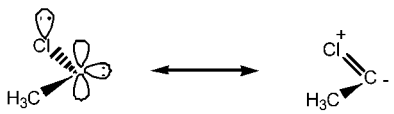

Keating et al. computed activation barriers of 11.5 and 10.9 kcal/mol for the 1,2-H migration using the B3LYP/6-311G**//B3LYP/6-31G* and MP2/6-31G* levels of theory, respectively.[5] For our calculations, singlet and triplet **CMC** were constrained in C_1 and C_s symmetry, respectively, and then fully optimized. These optimized geometries are depicted in Figure 3, and the relative energies are given in Table 3. Using the QCISD(T)/6-311+G**//B3LYP/6-31G* level, we calculate that the singlet state is 8.4 kcal/mol more stable than the triplet state. The additivity approximation increases the S−T energy separation to 10.5 kcal/mol.

Keating et al.[5] observed bystander effects when there is alkyl substitution on the methyl group bearing the migrating hydrogen. Chlorine, relative to hydrogen directly bonded to the carbene center, exerts a huge bystander effect on the 1,2-hydrogen migration reaction and is computed to raise the activation barrier to 13.1 kcal/mol at the QCISD(T)/6-311+G**//B3LYP/6-31G* level. The QCISD(T)/6-31+G(2d,p) additivity approximation is in agreement with this value and indicates that the barrier is 13.4 kcal/mol. Isodesmic reactions used to calculate the SSE of chlorine indicate that singlet methylcarbene is stabilized by nearly 19−20 kcal/mol upon substitution of H with Cl. This value is nearly 10 kcal/mol greater than the SSE of a methyl group, and is reflected in the increased barrier for the 1,2-hydrogen migration in **CMC** relative to **DMC**. Indeed, donation of the lone pair of electrons on chlorine into the empty p orbital of the carbene makes chlorine a better singlet stabilizer than alkyl substitution. On the other hand, an isodesmic reaction used to calculate the analogous triplet stabilization energy (TSE) indicated that the degree to which the triplet state of methylcarbene is stabilized upon substitution of H by Cl or CH_3 is identical (∼5 kcal/mol).

The experimentally determined barrier to the 1,2-H migration in chloromethylcarbene is 4.9 kcal/mol.[20]

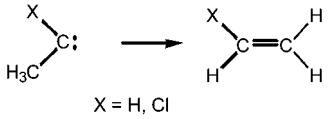

Based on Ford et al.'s[2] study of dimethylcarbene and dimethylcarbene-d_6, it seems likely that QMT contributes to the isomerization of chloromethylcarbene and lowers the apparent barrier accounting for the discrepancy between the calculated and measured values.

It has been experimentally demonstrated that chloroethylcarbene and chloroisopropylcarbene isomerize much more rapidly than does chloromethylcarbene.[9,20] Methyl substitution α to the migrating hydrogen lowers the C−H bond dissociation energy and stabilizes the developing positive charge that occurs on the carbon bearing the migrating hydrogen in the transition state.[21]

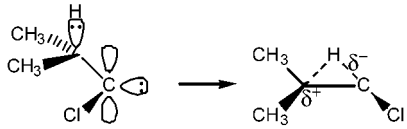

III.4. *tert*-Butyl Substituted Carbenes. *tert*-Butylcarbene (**TBC**) rearranges by a 1,3-C−H insertion (process A) or a 1,2-methyl migration (process B). Process A is the major pathway

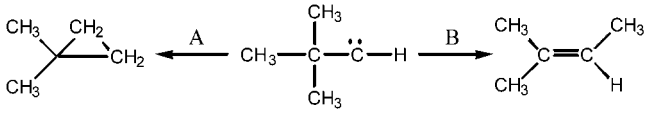

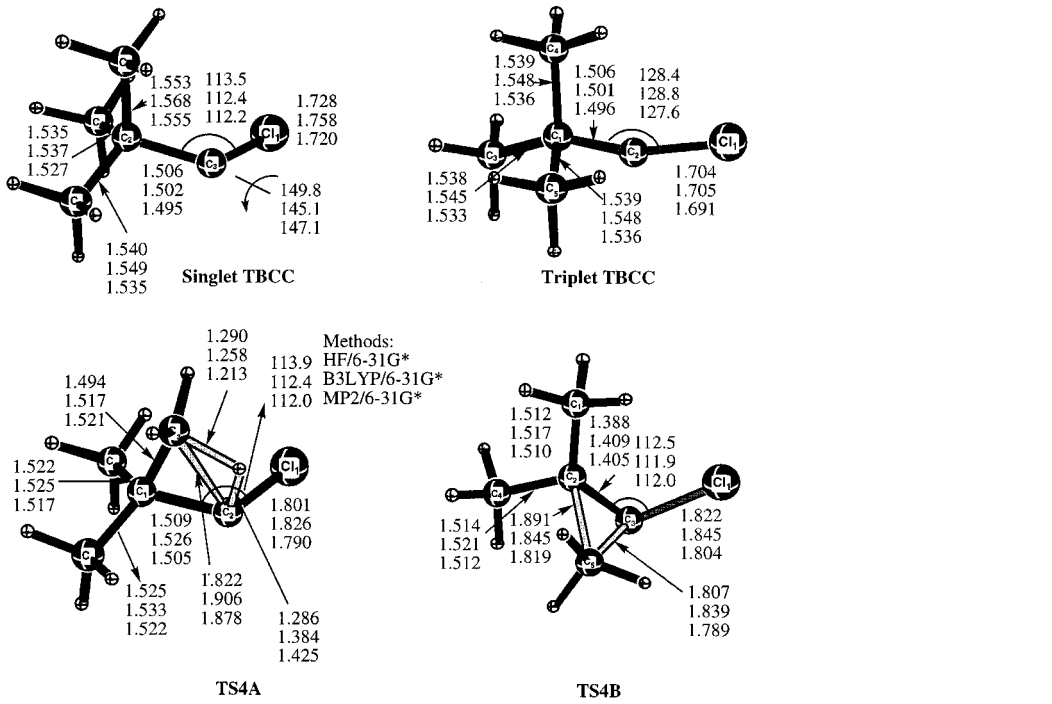

Figure 4. Optimized structures and some geometric parameters for *tert*-butylchlorocarbene (**TBCC**). Bond distances are in Å, and angles are in degrees.

TABLE 4: Calculated Relative Energies (kcal/mol) of *tert*-Butylchlorocarbene (TBCC)[a]

	HF/6-31G*	MP2/6-31G*	B3LYP/6-31G*	MP2/6-31+G(2d,p)	QCISD(T)/6-31G*//MP2/6-31G*[b]	QCISD(T)/6-31+G(2d,p)[c]
TBCC-S (C_1)	0.0	0.0	0.0	0.0	0.0	0.0
TBCC-T (C_1)	−15.9	3.0	5.7	7.1	5.3	9.3
TS4A (C_1)	23.6	9.5	10.6	8.2	13.3	11.9
TS4B (C_s)	20.2	10.2	10.7	8.9	14.6	13.4
A (C_s)	−50.2	−60.8	−55.5	−54.7	−53.8	−47.7
B (C_1)	−58.6	−67.4	−64.1	−63.8	−62.8	−59.2

[a] Relative energies include scaled zero-point vibrational energy (ZPVE) corrections and are reported at 0 K. Enthalpies at 298 K relative to **TBCC**-S at the HF/6-31G(d), B3LYP/6-31G(d), and MP2/6-31G(d) levels are listed in the Supporting Information. See Figure 4 for structures. [b] Single-point energies include ZPVE computed at the MP2/6-31G* level. [c] The relative energies at QCISD(T)/6-31+G(2d,p) were computed using the additivity approximation: $\Delta E = \Delta E$[QCISD(T)/6-31G*//MP2/6-31G*] + ΔE[MP2/6-31+G(2d,p)] − ΔE[MP2/6-31G*] and include the scaled MP2/6-31G* ZPVE corrections.

in the gas phase.[22] Although solvent dramatically influences the observed ratio of 1,1-dimethylcyclopropane to trimethylethylene,[23] bimolecular chemistry of **TBC** has not been reported. Attempts to study **TBC** by the pyridine ylide method have so far been unsuccessful, indicating that the lifetime of this carbene is very short ($\tau \ll 100$ ps).[24]

These results are consistent with the calculations of Armstrong, McKee, and Shevlin (AMS).[25] Using the QCISD(T)/6-31+G(2d,p)//MP2/6-31G* level of theory, they computed that the barriers to 1,3-C−H insertion and 1,2-methyl migration, are 0.1 and 3.7 kcal/mol, respectively, after zero-point energy correction. It was not necessary for us to perform calculations on **TBC**, due to the thorough study already described in the literature. AMS found that the S−T energy gap of **TBC** is 3.4 kcal/mol, with the triplet being the ground state.[25]

Although we have not performed calculations on **TBC,** we have studied *tert*-butylchlorocarbene (**TBCC**) and *tert*-butylmethylcarbene (**TBMC**) by computational methods to examine bystander effects on the rearrangements of *tert*-butyl substituted carbenes.

tert-Butylchlorocarbene. Once again, a chlorine substituent exerts an enormous bystander effect. **TBCC** is a relatively long-lived carbene in solution ($\tau > 90$ ns).[20,26a] It undergoes efficient bimolecular chemistry in a manner reminiscent of chloromethylcarbene. Moss and co-workers have determined that the absolute rate constants for processes A and B are 6.9×10^5 and 2.4×10^5 s^{-1}, respectively, at ambient temperature in isooctane.[26b]

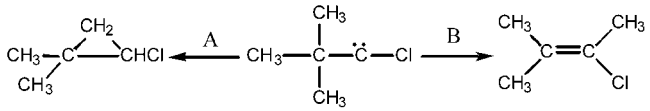

TBCC

The optimized geometries and selected parameters of **TBCC** are shown in Figure 4. Singlet **TBCC** has C_1 symmetry and the dihedral angle Cl−C−C−C is 149.8°, 145.1° and 147.1° at the HF/6-31G*, B3LYP/6-31G* and MP2/6-31G* levels. Triplet **TBCC** has C_1 symmetry. As expected, the C−C−Cl bond angle of singlet **TBCC** (112.2°) is smaller than that of triplet **TBCC** (127.6°) but is larger than that of singlet **MC** (105.6°) for steric reasons at the MP2/6-31G* level of theory. Similarly, the calculated bond angle at the carbene center of singlet **TBC** (111.8°) is larger than that of singlet **MC** (105.6°). Nevertheless, at the MP2/6-31G* level, triplet **TBCC** has a carbene bond angle (127.6°) that is smaller than that of triplet **MC** (131.6°) because of the electronegativity of the chlorine atom and its

TABLE 5: Calculated Relative Energies (kcal/mol) of Singlet and Triplet *tert*-Butylmethylcarbene (TBMC) Conformers[a]

	HF/6-31G*	MP2/6-31G*	B3LYP/ 6-31G*	MP2/6-31+ G(2d,p)	QCISD(T)/6-31G*// MP2/6-31G*[b]	QCISD(T)/6-31+ G(2d,p)[c]
TBMC-anti-(C_1) singlet	0.0	0.0	0.0	0.0	0.0	0.0
TBMC-syn-(C_1) singlet	0.8	1.1	0.9	1.3	0.9	1.1
TBMC-anti-(C_s) singlet	2.3	3.8	3.5	3.4	2.7	2.2
TBMC-syn-(C_s) singlet	0.8	1.4	1.2	1.7	0.9	1.1
TBMC-anti-(C_s) triplet	−22.9	−6.2	−3.1	−2.0	−4.1	0.1
TBMC-syn-(C_s) triplet	−22.0	−5.2	−2.4	−1.0	−3.2	1.1

[a] Relative energies include scaled zero-point vibrational energy (ZPVE) corrections and are reported at 0 K. Enthalpies at 298 K relative to **TBMC**-anti-(C_1) at the HF/6-31G(d), B3LYP/6-31G(d), and MP2/6-31G(d) levels are listed in the Supporting Information. See Figure 5 for structures. [b] Single-point energies include ZPVE computed at the MP2/6-31G* level. [c] The relative energies at QCISD(T)/6-31+G(2d,p) were computed using the additivity approximation: $\Delta E = \Delta E$[QCISD(T)/6-31G*//MP2/6-31G*] + ΔE[MP2/6-31+G(2d,p)] − ΔE[MP2/6-31G*] and include the scaled MP2/6-31G* ZPVE corrections.

TABLE 6: Calculated Relative Energies (kcal/mol) of *tert*-Butylmethylcarbene (TBMC) and Related Transition States and Products Formed upon Rearrangement[a]

	HF/6-31G*	MP2/6-31G*	B3LYP/ 6-31G*	MP2/6-31+ G(2d,p)	QCISD(T)/6-31G*// MP2/6-31G*[b]	QCISD(T)/6-31+ G(2d,p)[c]
TBMC-anti-(C_1) singlet	0.0	0.0	0.0	0.0	0.0	0.0
TBMC-anti (C_s) triplet	−22.9	−6.2	−3.1	−2.0	−4.1	0.1
TS5A (C_1)	19.5	4.2	6.2	3.3	7.4	6.6
TS5B (C_1)	21.0	7.1	8.7	6.1	11.3	10.3
TS5C (C_1)	17.5	5.7	7.9	4.1	8.4	6.8
product A	−57.3	−71.9	−64.0	−66.2	−65.4	−59.6
product B	−63.4	−75.5	−71.9	−72.0	−71.6	−68.1
product C	−62.2	−74.6	−67.6	−72.5	−70.7	−68.6

[a] Relative energies include scaled zero-point vibrational energy (ZPVE) corrections and are reported at 0 K. Enthalpies at 298 K relative to **TBMC**-anti-(C_1) at the HF/6-31G(d), B3LYP/6-31G(d), and MP2/6-31G(d) levels are listed in the Supporting Information. See Figure 6 for structures. [b] Single-point energies include ZPVE computed at the MP2/6-31G* level. [c] The relative energies at QCISD(T)/6-31+G(2d,p) were computed using the additivity approximation: $\Delta E = \Delta E$[QCISD(T)/6-31G*//MP2/6-31G*] + ΔE[MP2/6-31+G(2d,p)] − ΔE[MP2/6-31G*] and include the scaled MP2/6-31G* ZPVE corrections.

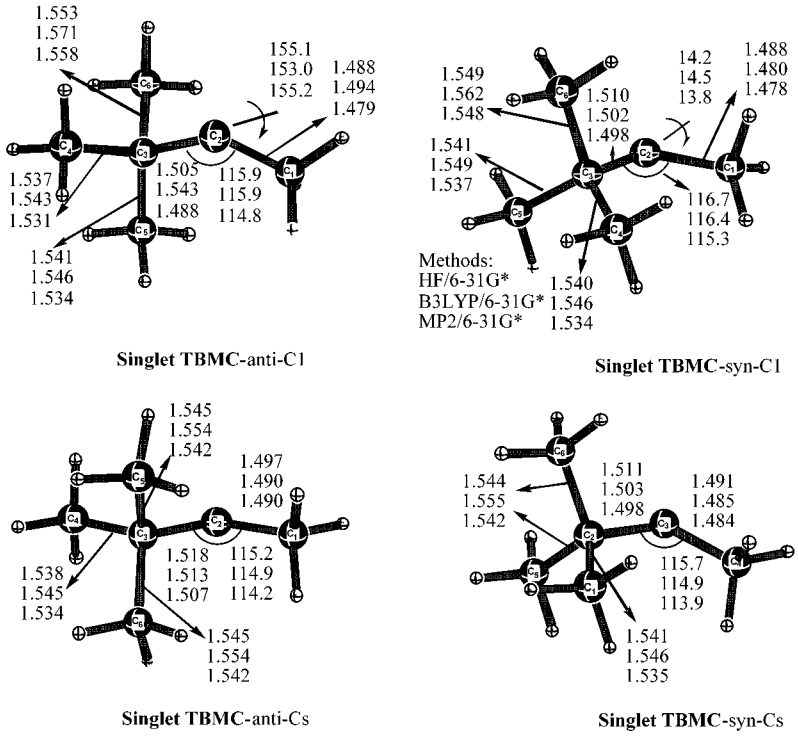

Figure 5. Optimized structures and some geometric parameters of the different conformers of singlet *tert*-butylmethylcarbene (**TBMC**). Bond distances are in Å, and angles are in degrees.

preference to form bonds to carbon rich in p character, despite the steric effect.

The relative energies of singlet and triplet **TBCC** are given in Table 4. It is very computationally demanding to study **TBCC** using a triple-ζ basis set and higher theoretical levels. Therefore, we calculated the S−T energy separation and the activation energies by using an additivity approximation.[10c,d] The S−T energy separation is −9.3 kcal/mol and the barriers to pathways A and B are 11.9 and 13.4 kcal/mol, respectively. It is clear that α-chlorine not only exerts a bystander effect on the 1,2-H migration, but also on the 1,3-C−H insertion and 1,2-methyl migration in *tert*-butyl substituted carbenes.

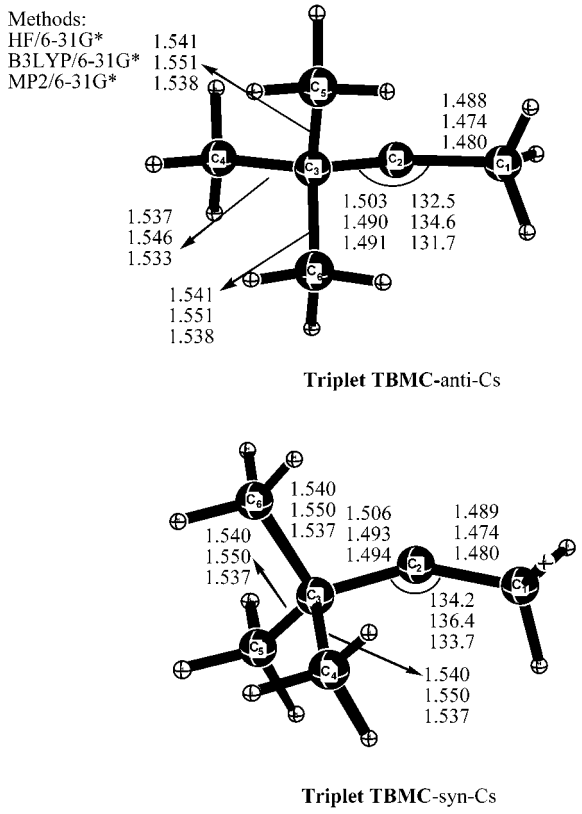

Figure 6. Optimized structures and some geometric parameters of the carbene conformers of triplet *tert*-butylmethylcarbene (**TBMC**). Bond distances are in Å, and angles are in degrees.

tert-Butylmethylcarbene (TBMC). **TBMC** can rearrange by 1,3-C−H insertion (A), 1,2-methyl migration (B), or 1,2-hydrogen migration (C). Pyrolysis of diazirine or tosyl hydrazone salt precursors leads to the products of processes A and C in proportions of 48:51 and 47:52, respectively. The 1,2-methyl migration product is formed in only trace amounts.[27] Similarly, photolysis of the diazirine forms products A and C in proportions of 33:53.[27]

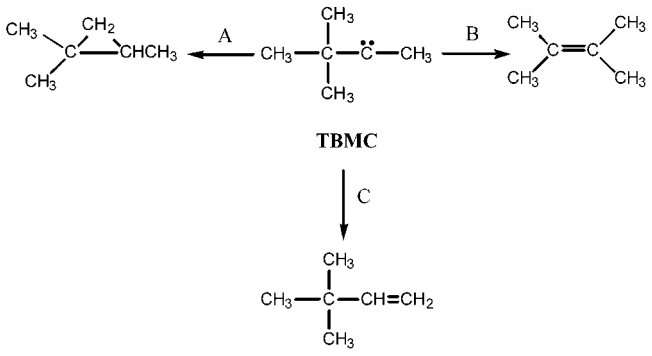

tert-Butylmethylcarbene has many possible conformations, six of which have been considered. Their relative energies are listed in Tables 5 and 6, and the optimized geometries are shown in Figures 5 and 6. Triplet **TBMC**-syn-(C_s) has one imaginary frequency, while singlet **TBMC**-anti and **TBMC**-syn-(C_s) each have two imaginary frequencies. The most stable singlet and triplet conformers of **TBMC** are singlet-anti-(C_1) and triplet-anti-(C_s), each with zero computed imaginary vibrational frequencies. All methods, including the additivity approximation, suggest a triplet ground state for **TBMC**. In contrast, the additivity approximation indicates that **DMC** is a ground-state

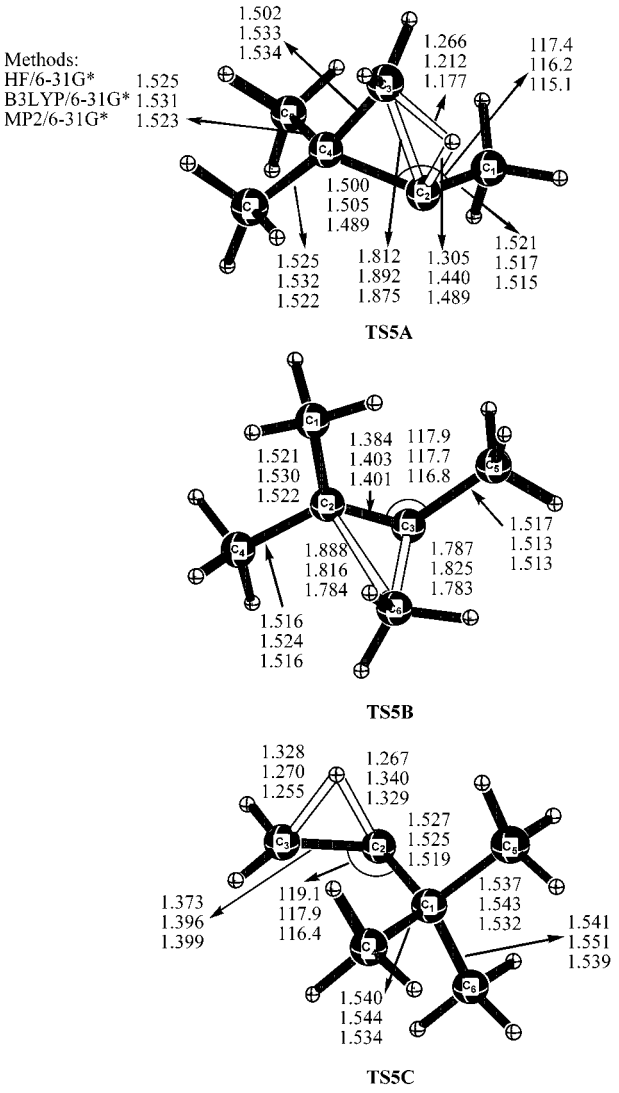

Figure 7. Optimized structures and some geometric parameters of *tert*-butylmethylcarbene (**TBMC**) transition states. Bond distances are in Å, and angles are in degrees.

singlet by 1.4 kcal/mol. This deviation between methyl substitution and *tert*-butyl substitution is explained by examining the isodesmic calculations of the SSEs. At all levels of theory, methyl substitution stabilizes the singlet state relative to methylcarbene more than *tert*-butyl substitution by 1−2 kcal/mol. Hence **DMC** is a ground-state singlet.

The difference between the two substituents is due to steric effects. The carbene bond angle of singlet **DMC** is 110.7° at the MP2/6-31G* level. In **TBMC**, steric repulsion increases the bond angle to 114.8°. Singlet **DMC** is 2−3 kcal/mol lower in energy than the triplet state. Steric effects differentially destabilize singlet **TBMC** and renders the singlet and triplet states to be about the same in energy. Indeed, the additivity approximation at QCISD(T)/6-31+G(2d,p) produces the smallest S−T energy separation (−0.1 kcal/mol), suggesting a singlet ground state for **TBMC**. Indeed, the singlet and triplet states of **TBMC** are essentially degenerate.

The methyl group at the carbene carbon has a spectator effect on the rearrangements of the *tert*-butyl group, but it is smaller than that of a chlorine atom. The barrier to 1,3-C−H insertion (pathway A) is 6.6 kcal/mol, and the barrier to 1,2-methyl migration (pathway B) is 10.3 kcal/mol for **TBMC** at the QCISD(T)/6-31+G(2d,p) level. The rearrangement barriers of the *tert*-butyl group in **TBMC** (where CH_3 is the bystander

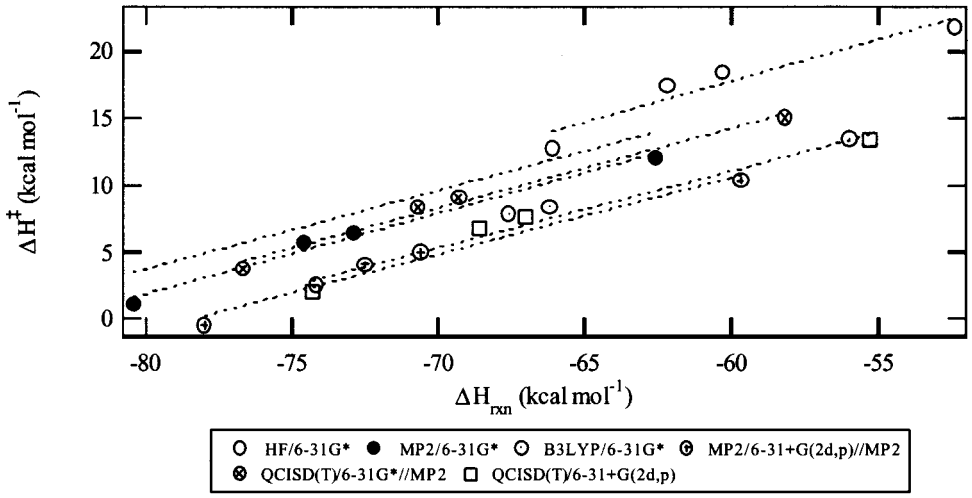

Figure 8. Plot of ΔH for 1,2-H migration versus $\Delta H^{\ddagger}$.

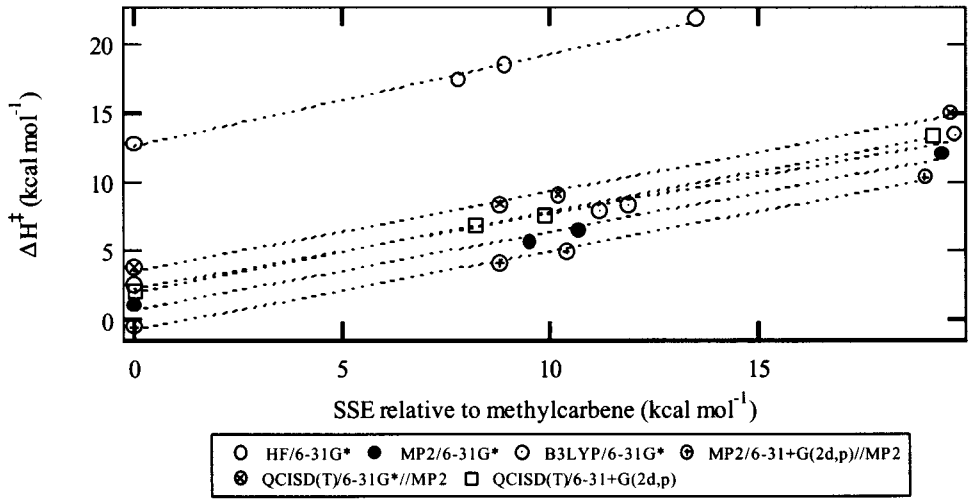

Figure 9. Plot of SSE relative to singlet methylcarbene versus $\Delta H^{\ddagger}$.

group) are both about 4 kcal/mol smaller than that of **TBCC** (where Cl is the bystander group) but are substantially larger than those of *tert*-butylcarbene. The barrier to 1,2-H migration of **TBMC** (pathway C) is 6.8 kcal/mol, about 0.6 kcal/mol less than that of dimethylcarbene. In both cases, CH_3 is the bystander group in the 1,2-H migration; however, the decreased barrier to 1,2-H migration in **TBMC** is likely due to the destabilization of **TBMC** from steric interactions.

IV. Discussion

Calculations indicate that there is a substantial bystander effect on the 1,2-migration of hydrogen in alkylcarbenes. The barrier to rearrangement increases for X = H < $C(CH_3)_3$ < CH_3 <

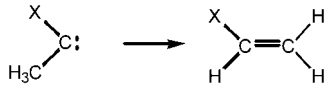

Cl. Similar increases in barrier heights are predicted in the rearrangements of *tert*-butyl groups attached to a carbene center. Previously, it has been shown that hyperconjugative interaction between alkyl groups and the carbene carbon can influence which pathway will dominate when multiple rearrangements are possible.[28]

As shown in Figure 8, Polanyi type plots of $\Delta H^{\ddagger}$ versus ΔH_{rxn} are roughly linear for each theoretical level. This can be understood with the aid of isodesmic reactions of singlet carbenes, which yield singlet stabilization energies (SSE's) as a function of X, where SSE = ΔH of the following reaction

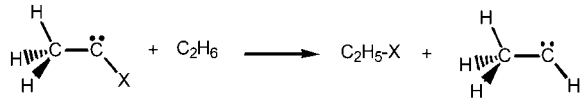

As shown in Figure 9, plots of SSE versus $\Delta H^{\ddagger}$ are linear with slopes of approximately 0.5−1.0, depending on the theoretical level. Thus, the increase in barrier height with X is largely due to the differential stabilization of the singlet carbene, relative to the transition state to rearrangement, by the substituent. This is also illustrated in Figure 10, which plots SSE relative to singlet methylene for the following isodesmic reaction

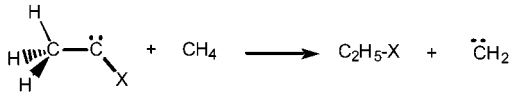

As expected, small substituent effects on the triplet state of methylene (Figure 11) do not correlate with the activation energy for 1,2-H migration. On the other hand, there remains fair correlation between the S−T energy separation and $\Delta H^{\ddagger}$ (Figure 12) since the S−T energy gap is affected to the greatest degree by the SSE (not the TSE) for the carbenes studied in this work.

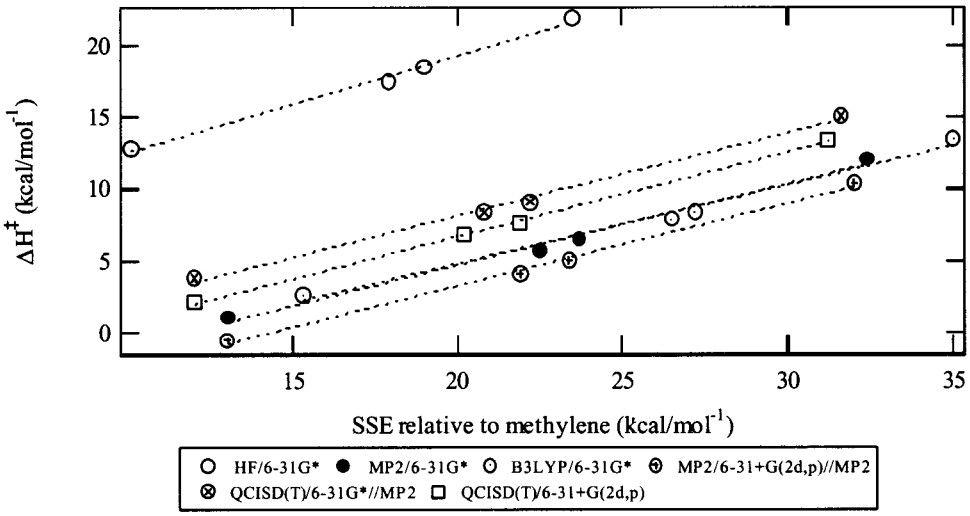

Figure 10. Plot of SSE relative to singlet methylene versus $\Delta H^{\ddagger}$.

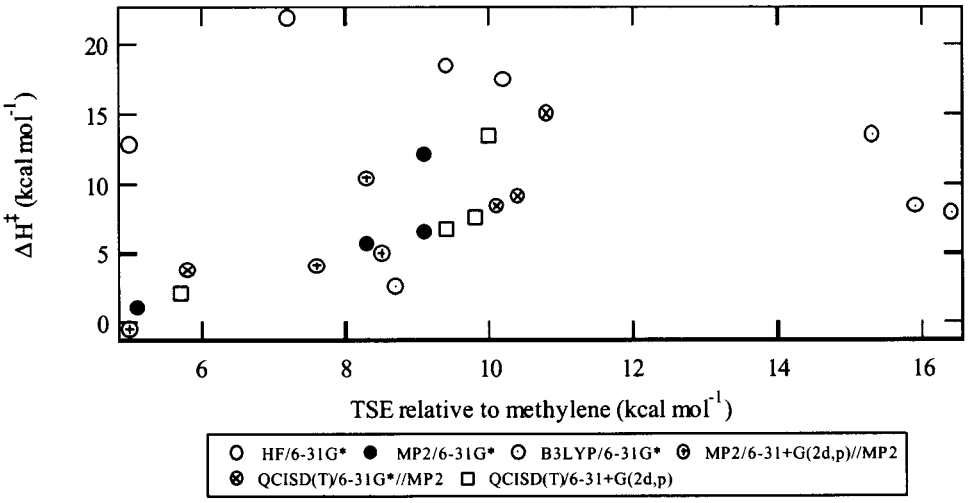

Figure 11. Plot of TSE relative to triplet methylene versus $\Delta H^{\ddagger}$.

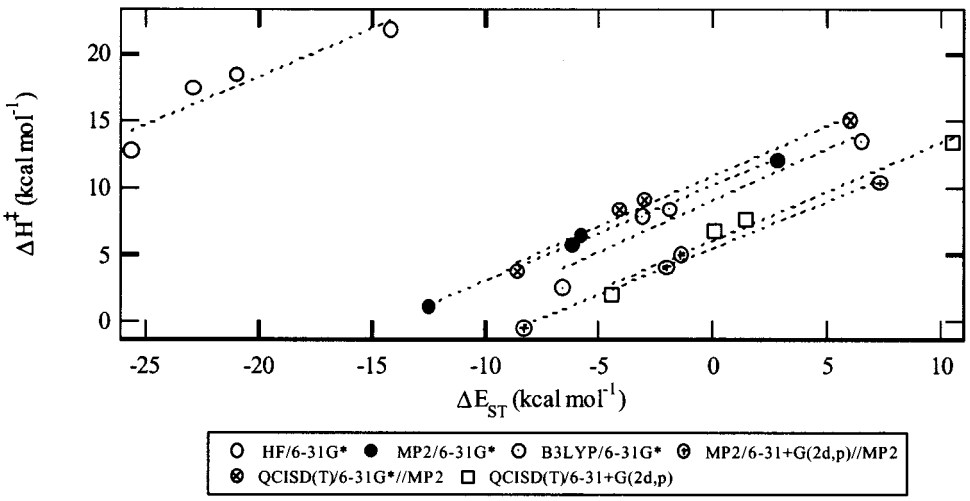

Figure 12. Plot of singlet−triplet energy separation versus $\Delta H^{\ddagger}$.

V. Conclusions

We have investigated the bystander effects on alkylcarbene rearrangements using both ab initio and density functional theory methods. The barriers to 1,2-hydrogen migration for $CH_3{-}C{-}X \rightarrow CH_2{=}CH{-}X$ were found to increase for X = H < CH_3 < $C(CH_3)_3$ < Cl. Isodesmic reactions indicate that the bystander group at the carbene center influences the magnitude of the activation barriers to rearrangement. Indeed, the function of the bystander group is to differentially stabilize the singlet states of the carbene reactant. The greatest singlet stabilization was observed when the bystander group is chlorine.

Acknowledgment. Support of this work by the NSF (CHE-9613861 and CHE-9733457) is gratefully acknowledged. Computational resources from the Ohio Supercomputer Center are gratefully acknowledged. One of us (B.T.H.) is pleased to acknowledge support of The Ohio State University Postdoctoral Fellowship.

Supporting Information Available: A full listing of the relative enthalpies at 298 K are tabulated. A complete listing of the electronic energies, Cartesian coordinates, and vibrational frequencies for each optimized structure is given in tabular format. This material is available free of charge via the Internet at http://pubs.acs.org.

References and Notes

(1) Baron, W. J.; DeCamp, M. R.; Hendrick, M. E.; Jones, M., Jr.; Levin, R. H.; Sohn, M. B. *Carbenes*; Wiley: New York, 1975; Vol. 1.

(2) Ford, F.; Yuzawa, T.; Platz, M. S.; Matzinger, S.; Fülscher, M. *J. Am. Chem. Soc.* **1998**, *120*, 4430−4438.

(3) Platz, M. S. *Adv. Carbene Chem.* **1998**, *2*, 133.

(4) Miller, D. M.; Schreiner, P. R.; Schaefer, H. F., III. *J. Am. Chem. Soc.* **1995**, *117*, 4137−4143.

(5) Keating, A. E.; Garcia-Garibay, M. A.; Houk, K. N. *J. Phys. Chem. A* **1998**, *102*, 8467−8476.

(6) (a) Bally, T.; Matzinger, S.; Truttmann, C.; Platz, M. S.; Morgan, S. *Angew. Chem., Int. Ed. Engl.* **1994**, *33*, 1964. (b) Ammann, J. R.; Subramanian, R.; Sheridan, R. S. *J. Am. Chem. Soc.* **1992**, *114*, 7592. (c) Modarelli, D. A.; Platz, M. S.; Sheridan, R. S.; Ammann, J. R. *J. Am. Chem. Soc.* **1993**, *115*, 10440−10441. (d) Pezacki, J. P.; Warkentin, J.; Wood, P. D.; Lusztyk, J.; Yazawa, T.; Gudmundsdöttir, A. D.; Morgan, S.; Platz, M. S. *J. Photochem. Photobiol. A* **1998**, *116*, 1. (e) Bonneau, R.; Hellrung, B.; Liu, M. T. H.; Wirz, J. *J. Photochem. Photobiol. A* **1998**, *116*, 9.

(7) (a) Gano, J. E.; Wottach, R.; Platz, M. S.; Senthilnathan, V. P. *J. Am. Chem. Soc.* **1982**, *104*, 2326. (b) Morgan, S.; Platz, M. S.; Jones, M., Jr.; Myers, D. R. *J. Org. Chem.* **1991**, *56*, 1351.

(8) Nickon, A. *Acc. Chem. Res.* **1993**, *26*, 84−89.

(9) (a) Liu, M. T. H. *J. Chem. Soc., Chem. Commun.* **1985**, 982. (b) La Villa, J. A.; Goodman, J. L. *J. Am. Chem. Soc.* **1989**, *111*, 6877−6878. (c) Liu, M. T. H.; Bonneau, R. *J. Am. Chem. Soc.* **1996**, *118*, 8098.

(10) (a) Frisch, M. J.; Trucks, G. W.; Schlegel, H. B.; Gill, P. M. W.; Johnson, B. G.; Robb, M. A.; Cheeseman, J. R.; Keith, T.; Petersson, G. A.; Montgomery, J. A.; Raghavachari, K.; Al-Laham, M. A.; Zakrzewski, V. G.; Ortiz, J. V.; Foresman, J. B.; Cioslowski, J.; Stefanov, B. B.; Nanayakkara, A.; Challacombe, M.; Peng, C. Y.; Ayala, P. Y.; Chen, W.; Wong, M. W.; Andres, J. L.; Replogle, E. S.; Gomperts, B.; Martin, R. L.; Fox, D. J.; Binkley, J. S.; Defrees, D. J.; Baker, J.; Stewart, J. P.; Head-Gordon, M.; Gonzalez, C.; Pople, J. A. *Gaussian 94*, Revision D.2; Gaussian Inc.: Pittsburgh, PA, 1995. (b) Scott, A. P.; Radom, L. *J. Phys. Chem.* **1996**, *100*, 16502. (c) McKee, M. L.; Lipscomb, W. N. *J. Am. Chem. Soc.* **1981**, *103*, 4673−4676. (d) Nobes, R. H.; Bouma, W. J.; Radom, L. *Chem. Phys. Lett.* **1982**, *89*, 497.

(11) Evanseck, J. D.; Houk, K. N. *J. Phys. Chem.* **1990**, *94*, 5518−5523.

(12) Khodabandeh, S.; Carter, E. A. *J. Phys. Chem.* **1993**, *97*, 4360−4364.

(13) Gallo, M. M.; Schaefer, H. F., III. *J. Phys. Chem.* **1992**, *96*, 1515−1517.

(14) Matzinger, S.; Fülscher, M. P. *J. Phys. Chem.* **1995**, *99*, 10747−10751.

(15) Ma, B.; Schaefer, H. F., III. *J. Am. Chem. Soc.* **1994**, *116*, 3539−3542.

(16) (a) Seburg, R. A.; McMahon, R. J. *J. Am. Chem. Soc.* **1992**, *114*, 7183. (b) Kramer, K. A. W.; Wright, A. N. *Tetrahedron Lett.* **1962**, 1095.

(17) Modarelli, D. A.; Platz, M. S. *J. Am. Chem. Soc.* **1993**, *115*, 470.

(18) Richards, C. A., Jr.; Kim, S.-J.; Yamaguchi, Y.; Schaefer, H. F., III. *J. Am. Chem. Soc.* **1995**, *117*, 10104−10107.

(19) Evanseck, J. D.; Houk, K. N. *J. Am. Chem. Soc.* **1990**, *112*, 9148−9156.

(20) (a) Bonneau, R.; Liu, M. T. H.; Rayez, M. T. *J. Am. Chem. Soc.* **1989**, *111*, 5973−5974. (b) Liu, M. T. H.; Bonneau, R. *J. Am. Chem. Soc.* **1989**, *111*, 6873−6874.

(21) Thamattoor, D. M.; Snoonian, J. R.; Sulzbach, H. M.; Hadad, C. M. *J. Org. Chem.* **1999**, *64*, 5886−5895.

(22) (a) Frey, H. M. *Adv. Photochem.* **1964**, *4*, 223. (b) Frey, H. M.; Stevens, I. D. R. *J. Chem. Soc.* **1965**, 3101. (c) Chang, K.-T.; Shechter, H. *J. Am. Chem. Soc.* **1979**, *101*, 508. (d) Fukushima, M.; Jones, M., Jr.; Brinker, U. *Tetrahedron Lett.* **1992**, 502.

(23) Ruck, R. T.; Jones, M., Jr. *Tetrahedron Lett.* **1998**, *39*, 2277.

(24) Platz, M. S.; Modarelli, D. A.; Morgan, S.; White, W. R.; Celebi, S.; Toscano, J. P. *Prog. React. Kinet.* **1994**, *19*, 93.

(25) Armstrong, B. M.; McKee, M. L.; Shevlin, P. B. *J. Am. Chem. Soc.* **1995**, *117*, 3685−3689.

(26) (a) Jackson, J. E.; Soundarajan, N.; Platz, M. S.; Liu, M. T. H. *J. Am. Chem. Soc.* **1988**, *110*, 5595. (b) Moss, R. A.; Liu, W. *J. Chem. Soc., Chem. Commun.* **1993**, 1597.

(27) (a) Flowers, M. C.; Frey, H. M. *J. Chem. Soc.* **1959**, 3953. (b) Moss, R. A.; Ho, G.-J. *J. Am. Chem. Soc.* **1990**, *112*, 5642−5644. (c) Zuev, P. S.; Sheridan, R. S. *J. Am. Chem. Soc.* **1994**, *116*, 4123−4124.

(28) (a) Sulzbach, H. M.; Platz, M. S.; Schaefer, H. F., III; Hadad, C. M. *J. Am. Chem. Soc.* **1997**, *119*, 5682−5689. (b) Xie, Y.; Schreiner, P. R.; Schleyer, P. v. R.; Schaefer, H. F., III. *J. Am. Chem. Soc.* **1997**, *119*, 1370. (c) Geise, C. M.; Hadad, C. M. *J. Am. Chem. Soc.* **2000**, *122*, 2863. (d) Mendez, F.; Garcia-Garibay, M. A. *J. Org. Chem.* **1999**, *64*, 7061. (e) Bettinger, H. F.; Schreiner, P. R.; Schleyer, P. v. R.; Schaefer, H. F. In *The Encyclopedia of Compuational Chemistry*; Schleyer, P. v. R., Allinger, N. L., Clark, T., Gasteiger, J., Kollman, P. A., Schaefer, H. F., Schreiner, P. R., Eds.; John Wiley and Sons Inc.: Chichester, U.K., 1998; pp 183−196. (f) Seburg, R. A.; Hill, B. T.; Squires, R. R. *J. Chem. Soc., Perkin Trans. 2* **1999**, *11*, 2249. (g) Armstrong, B. M.; McKee, M. L.; Shevlin, P. B. *J. Org. Chem.* **1998**, *63*, 7408. (h) Hu, J.; Hill, B. T.; Squires, R. R. *J. Am. Chem. Soc.* **1997**, *119*, 11699. (i) Poutsma, J. C.; Nash, J. J.; Paulino, J. A.; Squires, R. R. *J. Am. Chem. Soc.* **1997**, *119*, 4686. (j) Gleichmann, M. M.; Doetz, K. H.; Hess, B. A. *J. Am. Chem. Soc.* **1996**, *118*, 10551. (k) Bettinger, H. F.; Schleyer, P. v. R.; Schreiner, P. R.; Schaefer, H. F. *Modern Electronic Structure Theory and Applications to Organic Chemistry*; Davidson, E. L., Ed.; World Scientific Press Inc.: Singapore, 1997; pp 89−171. (l) Geise, C. M.; Hadad, C. M.; Zheng, F.; Shevlin, P. B. *J. Am. Chem. Soc.* **2002**, *124*, 355. (m) Geise, C. M.; Hadad, C. M. *J. Org. Chem.* **2000**, *65*, 8348.